Current Research in Food Science 8 (2024) 100743

Contents lists available at ScienceDirect

Current Research in Food Science

journal homepage: www.sciencedirect.com/journal/current-research-in-food-science

Intensification of rice flour gel structure by fermenting corresponding rice with *Lactobacillus plantarum*

Wenmin Ao [a], Likang Qin [a], Ning Wu [b], Pingzhen Ge [c], Chengmei Hu [a], Jinlan Hu [a], Yujie Peng [a], Yong Zhu [a,*]

[a] School of Liquor and Food Engineering, Guizhou University, Guiyang, 550025, PR China
[b] Zunyi Jinziyang Foods Co., Ltd, Zunyi, 563000, PR China
[c] Bijie Institute of Agricultural Sciences, Bijie, 551700, PR China

ARTICLE INFO

Handling Editor: Dr. Xing Chen

Keywords:
Lactobacillus plantarum
Rheology properties
Organic acid
Amylose
Rice gel

ABSTRACT

In starch gel foods processing, lactic acid fermentation is an effective strategy to improve the quality of the gel. This study revealed the effects of *Lactobacillus plantarum* fermentation for rice on the textural and rheological properties of the corresponding gels. The hardness, adhesiveness and chewiness of the gel showed ascending trends with the forwarding of fermentation. The role of *Lactobacillus plantarum* on rheological properties of gel depended on fermentation time. As the time was within 3 days, the process reduced the viscoelastic of the gel, while as the time was for 5 days, the process enhanced the viscoelastic of the gel. During fermentation, amylose content increased from 21.56 ± 1.17% to 27.39 ± 0.63%, and crude protein content descended from 12.60 ± 0.44 g/100 g DW to 4.8 ± 0.49 g/100 g DW. Total organic acids were ascending in the whole process, and lactic acid (LA), acetic acid (AA) and citric acid (CA) made the dominant contribution. The enthalpy change (ΔH) of the rice flour fermented for 5 days was significantly ($p < 0.05$) increased to 9.90 ± 0.24 J/g, indicating the formation of more double helix structures. These organic acids may contribute to the formation of the pores on the surface of granules by hydrolyzing the components, which provides a channel for enzymes to enter the interior of granules. These results provide the basis for the development of fermented rice-based foods.

1. Introduction

Rice is a staple food in China, containing starch, proteins, lipids, and minerals, and the starch accounts for 90% dry weight (DW) of polished rice. The starch gel is the main type of deep-processing product of rice (Amagliani et al., 2016), and the gel-forming is a crucial course for rice deep processing, consisting of gelatinization and retrogradation (Ulbrich et al., 2019). In the gelatinization stage, the starch granules are swelled in the presence of water under heating condition, which results in the destruction of starch structure and leaking of the amylose from starch granules, forming an amorphous starch paste (Dang et al., 2023). In the retrogradation stage, the destroyed starch is re-twined and aggregated with each other by means of hydrogen bonds, forming a three-dimensional network structure under cooling condition, and a large amount of water is blocked in the structure (Miles et al., 1985; Putseys et al., 2011). Amylose plays a crucial role in forming a gel network (Tian et al., 2023), and amylose content could serve as the indicator to evaluate the adaptability of the rice for producing gel-based foods, such as rice noodles (Wei et al., 2022), while protein negatively affected the forming of gels via hindering the connection of gel network (Wu et al., 2023).

Microbial fermentation is an effective strategy to improve the adaptability of ingredients, which could decrease the proportion of long amylopectin chains of sweet potato starch (Ye et al., 2019), and the fermentation process also provided a thicker texture to millet porridge (Zhang et al., 2024). In addition, lactic acid bacteria fermentation contributed to improving the tensile strength and overall eating quality of rice noodles (Yi et al., 2017).

The starch can form gels through the processes of gelatinization and retrogradation in the presence of water. During fermentation, the ratio of amylose and amylopectin was increased due to the starch degrading (Luo et al., 2022). In addition, protein and lipids were also degraded by microorganisms, which weakened their binding effects to starch, contributing to the enhancement of starch gel structure (Wang et al., 2022). *Lactobacillus plantarum*, the dominant bacteria in naturally fermented rice broth, was adopted in the production of fermented rice

* Corresponding author. School of Liquor and Food Engineering, Guizhou University, Huaxi District, Guiyang, 550025, PR China.
E-mail addresses: zhuyonghappycool@163.com, yzhu5@gzu.edu.cn (Y. Zhu).

https://doi.org/10.1016/j.crfs.2024.100743
Received 9 January 2024; Received in revised form 10 March 2024; Accepted 17 April 2024
Available online 18 April 2024

noodles (Geng et al., 2019; Lu et al., 2008), and it could exert function by generating metabolites, such as organic acids and oligosaccharides. The organic acids disrupted the ordered structure of starch and broke down starch granules, which contributed to the increasing hardness, chewiness and mouthfeel of rice noodles, whereas oligosaccharides (e.g., maltose) negatively affected the stretching and sensory properties of the rice noodles (Lu et al., 2008).

In the present study, the rice was initially subjected to the fermentation process implemented by *Lactobacillus plantarum*, and then it underwent a sequential procedure for preparing rice gel, subsequently, the evolution of textural and rheological properties of the gel was determined. The effects of *Lactobacillus plantarum* fermentation for rice flour on the properties of the corresponding rice gel were revealed by analyzing the chemical components of rice, the textural and rheological properties of the gel, and the organic acids profile of the fermentation broth. This study provided the basis for the development of fermented rice-based foods.

2. Materials and methods

2.1. Materials

The rice adopted in this study was Gui Chao rice, which was purchased from the local market (Guizhou, China). The *Lactobacillus plantarum* (No. 22141) was purchased from the China Industrial Culture Preservation Center (CICC).

2.2. Chemicals

The potato amylose was purchased from Sigma Chemical Co. (St. Louis, MO, USA). The maize amylopectin was purchased from Macklin Biochemical Technology Co. (Shanghai, China). Standards of oxalic acid, malic acid and tartaric acid were purchased from Yuanye Biotechnology Co., Ltd. (Shanghai, China), and lactic acid and citric acid were purchased from Solarbio Technology Co. (Beijing, China). Other reagents were analytical grade.

2.3. Preparation of fermented rice

The *Lactobacillus plantarum* was activated by the sequential procedures consisting of plate streaking and expanded culture (MRS liquid for 18 h) to acquire bacterial seed suspension (10^7 cfu/mL). One hundred grams of rice was rinsed with sterilized water thrice in a sterilized Erlenmeyer flask, which was subsequently mixed with 120 mL sterilized water and 6 mL bacterial seed suspension. Then, the mixture was placed in an incubator at 30 °C for fermentation. The fermented rice was collected when the time was at 0.5, 2, 3 and 5 days, respectively, each of which was rinsed with distilled water thrice prior to crushing. Then, the residue was collected by filtering process and subsequently dried in a drying oven (45 °C, 8 h), which was furtherly crushed and sieved (100 mesh sieve). These fermented rice flours, named $F_{0.5}$, F_2, F_3, and F_5, were stored at 4 °C for further study. The rice flour without fermentation was served as the control (F_0). The fermentation broth was also collected when the time was at 0, 0.5, 2, 3 and 5 days for organic acid profile analysis.

2.4. Determination of textural properties of rice flour gel

An appropriate amount of rice flour suspension (15:85, w/w) was placed in a square mold box (2.5 cm × 2.5 cm × 2.5 cm), which was orderly subjected to steaming (30 min) and cooling procedures, and then it was stored in a refrigerator (4 °C, 24 h) to form a gel. The gel was prepared in triplicate. The textural properties were monitored using a physical property analyzer (CT3, Middleboro, MA, USA) (Tian et al., 2023). The TA10 cylindrical probe carried out the analysis starting from the center of the gel (warming up to room temperature prior to analysis). The maximum test target distance was 5.0 mm with a trigger point load of 5.0 g and a test speed of 1.0 mm/s, and the determination was implemented twice in a cycle. The hardness, adhesiveness, cohesiveness and chewiness were calculated from the TPA curves using Brookfield Texture Analyzer software.

2.5. Solubility and swelling power of rice flour

Rice flour (0.2 g, W_0) was mixed with 10 mL distilled water in a centrifuge tube, which was heated (90 °C, 30 min) in a water bath and mixed by a vortex every 2 min. The mixture was subjected to the centrifuging process (2000 g, 10 min) prior to cooling to room temperature using tap water. And then the supernatant was collected in a constant-weight Petri dish, which was dehydrated to constant weight (W_1) in an oven (105 °C), and the sediment adhered to the wall of the centrifuge tube was also weighted (Ws), and all samples were processed in triplicate. The solubility (S) and swelling power (SP) were calculated by referring to Eq. (1) and Eq. (2).

$$S\ (\%) = \frac{W_1}{W_0} \times 100 \tag{1}$$

$$SP\ (\%) = \frac{W_s}{W_0 \times \left(1 - \frac{S}{100}\right)} \tag{2}$$

2.6. Determination of rheological properties of rice flour gel

The rheological properties were determined using a DHR-1 rheometer (Waters, America) with a geometric parallel plate (40 mm diameter) and a Peltier temperature control system. Rice flour was mixed with distilled water to prepare a 15:85 (w/w) suspension. The mixture underwent the processes consisting of heating in a boiling water bath (30 min) and cooling in tap water to prepare the rice flour gel, and these gels prepared from rice flour fermented 0, 0.5, 2, 3, 5 days were named G_0, $G_{0.5}$, G_2, G_3 and G_5, respectively. An appropriate dimension of gel was placed on the center of the test bench of the rheometer using a spoon, and then the fixture was lowered to the gap of 1000 μm prior to scraping off excess sample. Data was collected using the Trios software. The evolution of storage modulus (G′, Pa), loss modulus (G″, Pa), loss tangent (tan δ), and complex viscosity (η*, Pa·s) was plotted in the angular frequency range between 0.6 and 100 rad/s at 25 °C with 1% strain.

2.7. Determination of dynamic viscosity of rice flour during gelatinization

The evolution of the dynamic viscosity of rice flour during gelatinization was monitored by referring to the methods reported by Mohammad Amini et al., 2015 and Irani et al. (2019) with slight modifications. An appropriate amount of rice flour suspension (15:85, w/w) was placed on the center of the test bench of the rheometer and the gap between the plates of the bench was adjusted to1000 μm, which was sealed by a layer of silicone oil. At a strain of 1% and an angular frequency of 6.283 rad/s, the temperature was initialed from 50 °C to 95 °C with a rate of 5 °C/min, and then it was cooled down to 25 °C at the same rate. Suspension samples were tested in triplicates. The evolution of dynamic viscosity with the extension of gelatinization temperature and time was collected using the Trios software.

2.8. Analysis of the organic acid profile of fermentation broth

The fermentation broth samples were sequentially subjected to centrifugating (10 min, 14,490 g) and filtering (0.22 μm, aqueous filter membrane) processes. Twenty microliter of the filtered broth was pipetted for HPLC analysis, in which the organic acids were separated by using a silicone-based column (ZORBAX SB-Aq, USA) at 25 °C coupled with isocratic elution using potassium dihydrogen phosphate (0.02 mol/

L, pH = 2.37) (98%) and methanol (2%) with the flow rate at 0.6 mL/min. These individual organic acids were determined by using the UV detector with a wavelength of 230 nm. Standards of lactic acid (LA), acetic acid (AA), oxalic acid (OA), tartaric acid (TA), malic acid (MA), and citric acid (CA) were adopted for identifying and quantifying these organic acids in fermentation broth.

2.9. Determination of nutritional components for rice flour

Total starch was determined by referring to the National Food Safety Standards of China, GB 5009.9 (China and Administration, 2016a). Rice flour was initially processed by removing fat and soluble sugar, and then it was sequentially subjected to a series of steps including gelatinization, saccharification, acid hydrolysis and neutralization. Finally, the total starch was calculated by titrating the alkaline copper tartrate solution using a sample.

The amylose content was determined by referring to the previous study (Tian et al., 2023). Rice flour was defatted using methanol (85% v/v) prior to dissolving in a sodium hydroxide solution (1 mg/mL) and gelatinization process. The series standard solutions were prepared by mixing amylose and amylopectin with 0.9 mol/L sodium hydroxide solution, in which the amylose content was from 10% (w/w) to 35% (w/w). The standard solution (5 mL) was mixed with acetic acid solutions (1 mL, 1 mol/L) and iodine reagent (2 mL) for the coloration reaction, and then the absorbance of the mixture was measured at 720 nm, the sample was processed the above procedures. The amylose content in the sample was calculated from the standard curve.

Crude protein content was determined by referring to the National Food Safety Standards of China, GB 5009.5 (China and Administration, 2016b). The sample (0.3 g) was decomposed by heating in the presence of copper sulfate (0.1 g), potassium sulfate (1 g) and sulfuric acid (5 mL). Different concentrations of ammonia nitrogen standard solution mixed with sodium acetate buffer solution (pH 4.8) and color developer (15 mL of formaldehyde mixed with 7.8 mL of acetylacetone and water to 100 mL) in the colorimetric tubes were heated prior to measuring the absorbance at 400 nm, and the standard curve was plotted by fitting these points indicating the concentration and the corresponding absorbance in the coordinates. The same procedure was performed for the samples, and the results were calculated from the standard curve and expressed as g/100 g DW.

2.10. Determination of thermal characteristics of rice flour

The thermal characteristics of rice flour were determined using the differential scanning calorimeter (DSC) (Q2000, TA Instruments, Inc., Newcastle, DE, USA). The rice flour (3.0 mg) was mixed with distilled water (6.0 μL) in a crucible. The mixture was subsequently sealed before equilibrating for 3 h at room temperature, and the sample was heated from 30 °C to 100 °C at the rate of 10 °C/min. The evolution of heat flow with the increasing temperature was monitored, and the onset temperature (To), peak temperature (Tp), conclusion temperature (Tc) and enthalpy change (ΔH) were calculated using the TA Universal Analysis software (TA Instruments, Newcastle, DE, USA). All samples were tested in triplicate.

2.11. Measurement of the microstructure of fermented rice flour

The fermented rice flour obtained from Section 2.3 was initially dried by using a drying oven (45 °C, 5 h). The surface of dried flour was sprayed with gold on the specimen stakes, which was subsequently examined by using a benchtop scanning electron microscope (EM-30, Coxem, South Korea). The images were captured at the magnification of 5000×.

2.12. Statistical analysis

The observed values were presented as means ± standard deviation (n = 3). One-way ANOVA test and Duncan multiple comparisons were performed to determine the differences between groups with different fermentation times at the level of 0.05 using SPSS 26.0 software (SPSS Inc., IL, USA).

3. Results and discussions

3.1. Textural properties of rice flour gel

For gel products, textural properties consist of hardness, adhesiveness, chewiness and cohesiveness (Dan et al., 2022; Nie et al., 2019). The hardness and adhesiveness are the main factors when customers select a product (Li et al., 2016), and adhesiveness value indicates the property sticking to teeth after chewing (Dou et al., 2023). The cohesiveness is related to the strength between gel molecules, while the chewiness indicates the ease when a product is chewed. In the present study, the hardness and chewiness of these rice flour gels showed ascending trends in the whole fermentation process, the adhesiveness of the gel showed a trend of decreasing first and increasing subsequently in the whole fermentation process, while the cohesiveness of these rice flour gels showed the opposite trend to adhesiveness in the whole fermentation process, as shown in Fig. 1. These suggested that the fermentation process for rice flour promoted the texture of the corresponding gel transforming into hard, sticky and chewy properties.

3.2. Solubility and swelling power of fermented rice flour

In the gel products process, such as rice noodles, solubility (S) and swelling power (SP) were important indicators to predict the consumer acceptability of products, and SP was positively correlated with the sensory score of products (Wei et al., 2022). This study presented the dynamic changes of S and SP of rice flour in the process fermented by *Lactobacillus plantarum*. The S and SP showed an increasing trend in the stage between 0 and 2 days, which increased to 8.63 ± 0.19% and 0.09 ± 0.00%, respectively, while, they showed a stable trend in the stage between 2 and 5 days, as shown in Fig. 2. The previous study suggested that S and SP were associated with both amylose content and amylopectin structure (Wei et al., 2022). The SP of starch relied on the water-holding capacity of starch molecules accomplished by hydrogen bonding (Li et al., 2020). Amylose played a vital role in the forming of gel network structures, and short amylopectin chains were also involved in the forming of gel network structures, which presented the capacity to bind free water (Sikora et al., 2019). The increased SP of the gel may originate from the degrading of amylopectin in the fermentation process, and the trends of S and SP in the latter stage may be associated with the ratio of amylopectin to amylose.

3.3. Rheological properties of rice flour gel

The storage modulus (G′) and loss modulus (G″) are adopted to evaluate the elasticity and viscosity of a gel. The G′ is positively associated with the elasticity of the gel, and the G″ indicates the viscosity of the gel. The complex viscosity (η*) represents the ability of a fluid resistance to deformation, which can be converted from G′ and G″ according to Eq. (3) (Han et al., 2016).

$$\eta^{*} = \frac{G^{''}\text{-}iG'}{\omega} \tag{3}$$

Where i indicates the imaginary unit, and ω indicates angular frequency.

The evolution of G′ and G″ with the increasing angular frequency was shown in Fig. 3 (A and B). The G′ and G″ gradually went up with the increasing angular frequency, and the G′ curves of $G_{0.5}$, G_2 and G_3 were

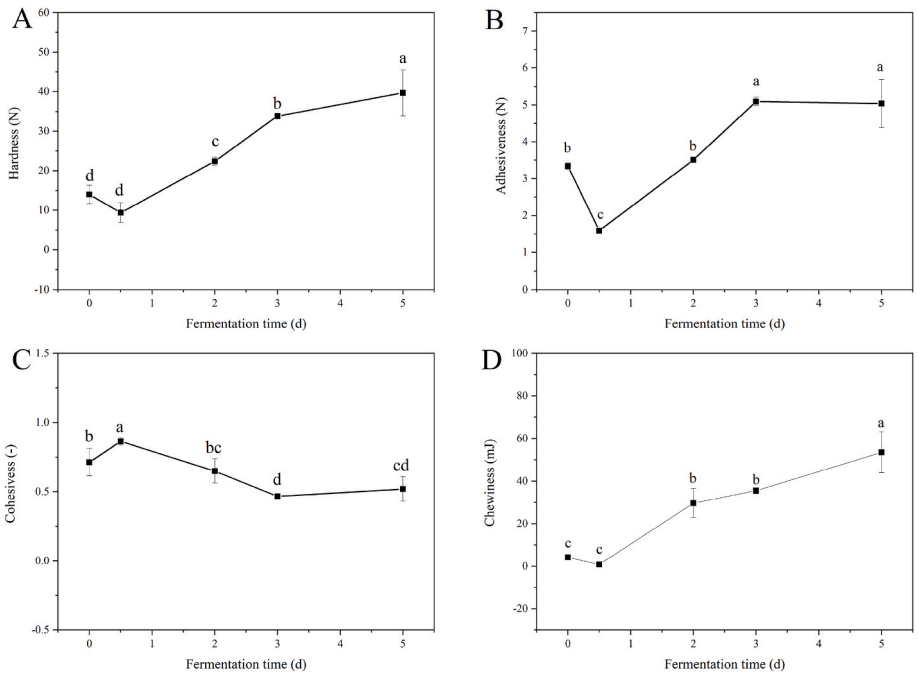

Fig. 1. The evolution of textural properties of the gel with the forwarding of fermentation for rice flour. Values with different lowercase letters indicate significant difference ($p < 0.05$). A indicates the hardness. B indicates adhesiveness. C indicates cohesiveness. D indicates chewiness.

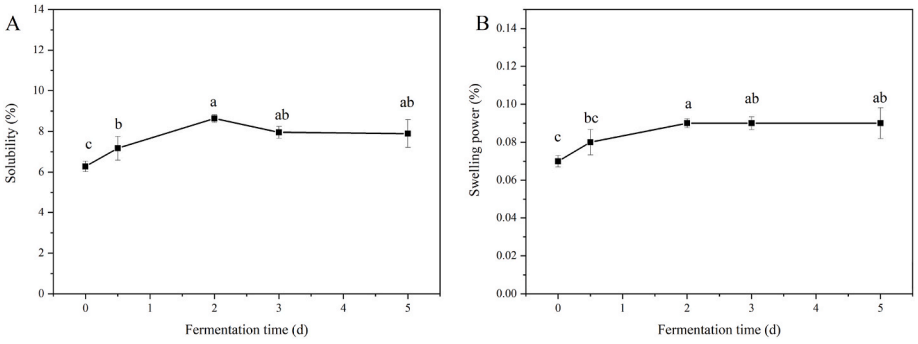

Fig. 2. The evolution of solubility (A) and swelling power (B) of rice flour with the forwarding of fermentation. Values with different lowercase letters indicate significant difference ($p < 0.05$).

arranged below the control curve; while the G′ curve of G_5 was arranged above the control curve. The G″ curves showed an overall ascending trend with the enlarging of angular frequency (ω), and the G'' (ω = 6 rad/s) of the G_5 was 1.3 times of the G_0. The G′ curves were arranged in the upper of the G″ curves. The loss tangent (tan δ) was also used to characterize the viscoelastic behaviors of the gels (Fig. 3 C), which was calculated by dividing the G″ using G'. The tan δ of these gels ranged from 0.08 to 0.17. The previous study suggested that the gel presented elastic behavior when the tan δ was no more than 1 (Varela et al., 2016). This indicated that these gels exhibited a solid-like state.

The curves, exhibiting the evolution of η* with the increasing of ω (Fig. 3 D), showed linear descending trends, which presented a shear-thinning property (Irani et al., 2019). This indicated that the fluid was easy to fill, model, and leak (Jiang et al., 2013). The previous study suggested that the η* curve fitted the viscosity power-law model (Eq. (4)) (Holdsworth, 1971). Hence, the consistency coefficient (K*, Pa·s^n) and flow behavior index (n*) were obtained by fitting the η* and ω using Eq. (4).

$$\eta^* = K^* \omega^{n^*-1} \quad (4)$$

The K* was positively correlated with the elasticity of the gel, and the n* was positively correlated with the shear thinning behavior (Tian et al., 2023). In the present study, the K* decreased from 5389.79 ± 4.88 Pa·s^n to 3670.30 ± 5.20 Pa·s^n in the fermentation stage between 0 and 3 days, while it increased to 6882.84 ± 5.06 Pa·s^n when the fermentation time was on day 5, as shown in Table 1. The n* kept constant throughout the whole process.

The viscoelasticity of the gel was affected by the network structure (Chen et al., 2023). The previous study suggested that the viscoelasticity of starch gels showed an increased trend with the forwarding of fermentation progress (Wang et al., 2023). In fermentation progress, the disaccharides generated from microorganism metabolism were in favor of hindering the reaggregation of starch chains, reducing the viscosity and elasticity of the gel (Wang et al., 2016). Moreover, organic acids generated from microorganism metabolism promoted the degradation of starch molecules, which resulted in the reduction of cohesiveness, springiness and adhesiveness (Chen et al., 2017; Karma et al., 2022). These may be the reason why the viscoelasticity of gel was descending in the fermentation stage between 0 and 3 days. In the late stage of fermentation, the growth of microorganisms tended to be stable, and the disaccharides produced from metabolism were consumed by themselves. This may partly account for the phenomenon that the

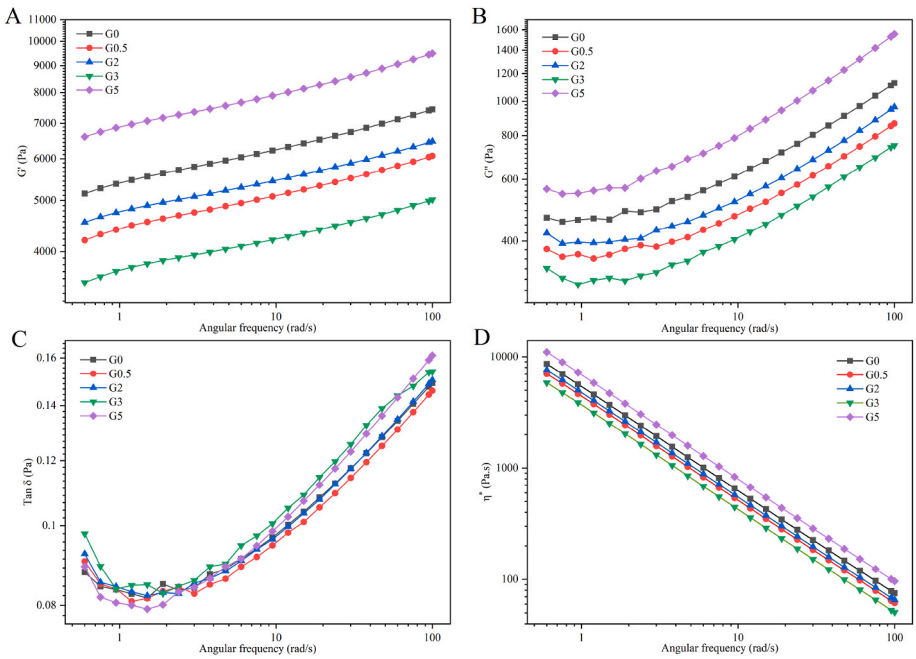

Fig. 3. The evolution of rheological properties of gels prepared by fermented rice flour with the increasing of angular frequencies. A indicates the energy storage modulus (G′). B indicates the loss modulus (G″). C indicates the loss tangent (tan δ). D indicates the dynamic viscosity (η*).

Table 1
Rheological parameters of fermented rice flour and corresponding gel.

Fermentation time (d)	T_s (°C)	T_{max} (°C)	η^*_{max} (Pa·s)	η^*_{min} (Pa·s)	η^*_f (Pa·s)	B (Pa·s)	SB (Pa·s)	K* (Pa·s^n)	n*
0	79.34 ± 0.26 ^{a}	89.67 ± 0.42 ^{a}	126.81 ± 8.35 ^{b}	0.05 ± 0.01 ^{b}	142.31 ± 5.33 ^{ab}	126.76 ± 8.36 ^{b}	142.26 ± 65.34 ^{ab}	5389.79 ± 4.88 ^{b}	0.07 ± 0.0017 ^{a}
0.5	77.76 ± 0.70 ^{b}	87.08 ± 1.83 ^{b}	171.89 ± 39.67 ^{a}	0.08 ± 0.01 ^{a}	187.83 ± 47.66 ^{a}	171.81 ± 39.65 ^{a}	187.75 ± 47.65 ^{a}	4408.40 ± 5.17 ^{d}	0.07 ± 0.0022 ^{a}
2	79.63 ± 0.31 ^{a}	89.40 ± 0.51 ^{a}	96.53 ± 13.66 ^{b}	0.05 ± 0.02 ^{b}	129.18 ± 22.55 ^{b}	96.49 ± 13.67 ^{b}	129.13 ± 22.56 ^{b}	4751.29 ± 4.59 ^{c}	0.07 ± 0.0018 ^{a}
3	79.62 ± 1.34 ^{a}	89.39 ± 0.56 ^{a}	101.66 ± 5.80 ^{b}	0.05 ± 0.02 ^{b}	132.84 ± 8.90 ^{b}	101.61 ± 5.78 ^{b}	132.80 ± 8.88 ^{b}	3670.30 ± 5.20 ^{e}	0.07 ± 0.0026 ^{a}
5	80.09 ± 0.26 ^{a}	89.87 ± 0.52 ^{a}	127.38 ± 13.44 ^{b}	0.04 ± 0.01 ^{b}	173.54 ± 19.35 ^{ab}	127.34 ± 13.45 ^{b}	173.50 ± 19.36 ^{ab}	6882.84 ± 5.06 ^{a}	0.07 ± 0.0014 ^{a}

Note: T_s indicates the temperature at which the η* was initially increasing. T_{max} indicates the temperature that the η* increased to the maximum value. η^*_{max} indicates the maximum value of η*. η^*_{min} indicates the minimum values of η*. η^*_f indicates the η* at 25 °C. B indicates the difference between η^*_{max} and η^*_{min}. SB indicates the difference between η^*_f and η^*_{min}. K* indicates the consistency coefficient. N* indicates the flow behavior index. Values with different lowercase letters within column indicate significant differences ($p < 0.05$).

viscoelasticity of G_5 was higher than the control.

3.4. Pasting properties of rice flour

In the gelatinizing process, the starch granules undergo a series of changes that consist of water absorbing, expanding, splitting, and gelatinizing (Irani et al., 2019; Zhu and Liu, 2020). The evolution of complex viscosity (η*) with the progress of heating (temperature and time) was monitored using a rheometer. The viscosity curves and rheological parameters were shown in Fig. 4 and Table 1, respectively. All samples shared the same trend. The η* was dynamically shifty in the whole process, which can be divided into four stages. In the first stage, the η* maintained at a low level, and then it passed into the second stage, in which the η* dramatically went up to the top peak (between 96.53 ± 13.66 Pa s and 171.89 ± 39.67 Pa s). Afterward, the η* showed a slight decline in the third stage, which decreased to the final complex viscosity (η^*_f). The η* showed a slight rise in the last stage. In the initial gelatinizing phase, the significant increase of viscosity ascribed to the process of absorbing water and swelling of starch granules (Ji et al., 2017; Rincón-Londoño et al., 2016), and then the starch particles were cracked under high temperature and mechanical shear stress, which eventually resulted in amylose leaching and arranging (Ahuja et al., 2020). This may account for the phenomenon in the third stage.

The breakdown viscosity (B) is defined as subtracting the minimum viscosity from the maximum viscosity, which can be used to measure the starch paste resistance to heat and shear, and the setback viscosity (SB) is the difference between η^*_f and η^*_{min}, which indicates the retrograde tendency of starch pastes (Fazeli et al., 2021; Irani et al., 2019). In the present study, the B and SB values of $G_{0.5}$ were higher than the other groups, which indicated that the rice flour fermented for 0.5 days presented a poor resistance to shear and more retrogradation tendencies. This was unfavorable in the processing of rice noodles.

3.5. The evolution of organic acid content during fermentation

Organic acids are vital metabolites of *Lactobacillus plantarum*. In this study, lactic acid (LA), acetic acid (AA), oxalic acid (OA), tartaric acid (TA), malic acid (MA) and citric acid (CA) were present in the fermentation broth, in which LA, AA, and CA were dominant, as shown in Fig. 5. In the fermentation process, the content of CA and LA showed

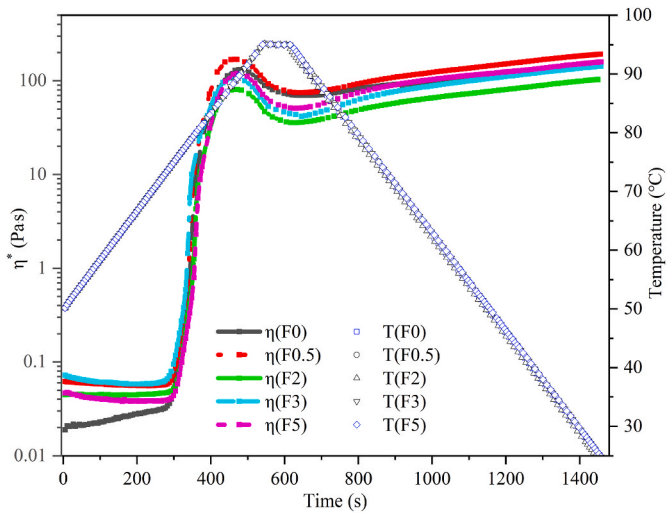

Fig. 4. The dynamic viscosity curves of fermented rice flour.

ascending trends, in which the CA content increased to 33.18 ± 5.55 mg/100 mL on day 5, and the LA content increased to 85.36 ± 5.76 mg/100 mL on day 5. The AA content showed a trend of ascending first and descending subsequently, which increased to the maximum value (81.63 ± 6.11 mg/100 mL) on day 2. Additionally, MA content showed an inverse trend compared with AA content, which initiated from 32.36 ± 8.02 mg/100 mL and decreased to the minimum value (8.43 ± 1.46 mg/100 mL) on day 3.

Lactobacillus plantarum is capable of producing LA, AA and other metabolites in the presence of available sugars, in which LA is the dominant constituent (Freire et al., 2017). With respect to the decreasing AA content in the stage between 2 and 5 days, this may originate from the inhibition effect of the high AA content on the metabolic pathway (Pinhal et al., 2019). TA, MA and CA were also detected in the metabolites of *Lactobacillus plantarum* (Xie et al., 2023).

In this study, the content of LA and CA gradually increased with the progression of fermentation, which coincided with the trend of hardness, adhesiveness and chewiness of gels, while the trend of AA was similar to the trend of cohesiveness of gels. This suggested that LA, AA and CA may be associated with the texture of gels. Zehra et al. suggested that the CA decreased the swelling index of sorghum and corn starch extrudates by strengthening the hydrogen bonding in the starch chain (Zehra et al., 2022). Organic acid also affected the viscosity of starch gels. The previous studies showed that gels prepared by the starch treated with organic acid (CA, LA, and AA) presented a lower viscosity than those prepared by raw starch (Hung et al., 2016; Majzoobi and Beparva, 2014). In addition, the gels prepared by AA and LA presented a softer texture with less adhesiveness, elasticity, cohesiveness, and chewiness (Majzoobi and Beparva, 2014). Furthermore, pea starch treated with MA presented an anti-digestive property (Shi et al., 2018). The present results showed that the fermentation process was in favor of

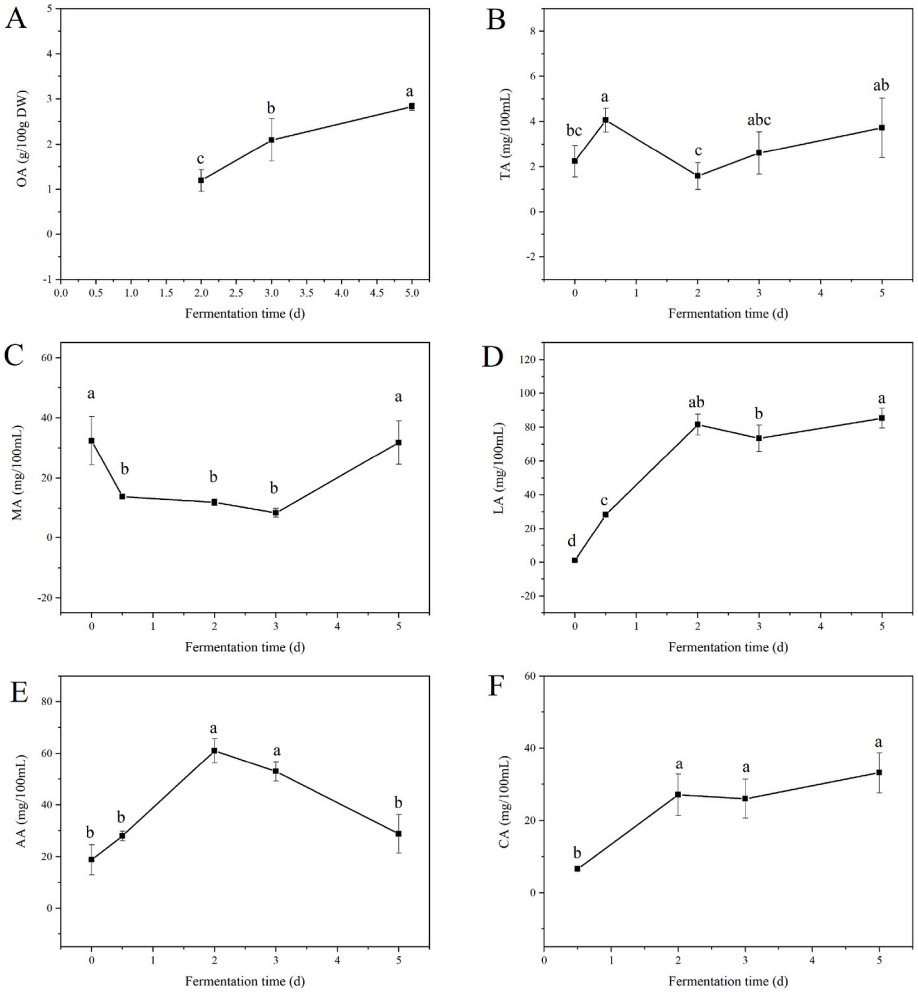

Fig. 5. The evolution of organic acid content in broth with the forwarding of fermentation. Values with different lowercase letters indicate significant difference ($p < 0.05$). A indicates oxalic acid. B indicates tartaric acid. C indicates malic acid. D indicates lactic acid. E indicates acetic acid. F indicates citric acid.

the generating of organic acids, which contributed to the improvement of the textural and functional properties of the gel.

3.6. The evolution of nutritional components of rice flour during fermentation

In the fermentation process, *Lactobacillus plantarum* fulfills its metabolism in the presence of rice substrate, which in turn modifies the chemical components of the substrate. The evolution of total starch, amylose and crude protein content in rice flour with the progression of fermentation was monitored. Total starch showed a slight decreasing trend, which ranged from 94.80 ± 1.28 g/100 g DW to 90.16 ± 1.48 g/100 g DW. Amylose content showed a significant increase in the stage a few hours after the start of fermentation until day 3, of which the maximum was at 27.39 ± 0.63%. The crude protein content showed a trend of increasing first and decreasing subsequently, which descended to 4.8 ± 0.49 g/100 g DW on day 5, as shown in Fig. 6.

In the rice fermentation process, the branched chain of amylopectin was degraded by metabolites, such as extracellular enzymes and acids (Lu et al., 2008; Tu et al., 2021). This may be responsible for the increasing trend of amylose content in the fermentation process. With regard to the evolution of crude protein content, we suggested that the partial protein in rice was transformed into water-soluble nitrogen by *Lactobacillus plantarum*, which was excluded from rice flour. The amylose constitutes the framework of the gel, which determines the gel properties. During fermentation, the changes in textural and rheological properties of gel partially ascribe to the increasing amylose content. Acids are in favor of the hydrolysis of starch (Punia et al., 2022). The present results demonstrated that both total organic acids and amylose content presented increasing trends with the forwarding of fermentation. This suggested that these organic acids contributed to the increased amylose content.

3.7. Thermal characteristics of rice flour

Thermal properties consist of gelatinization temperature and enthalpy change, and the evolution of To, Tp, Tc and ΔH of rice flour during fermentation was shown in Fig. 7. In this fermentation protocol, To, Tp and Tc of rice flour fermented by *Lactobacillus plantarum* were lower than that of unfermented rice flour. The Tc of rice flour ranged from 80.83 ± 0.58 °C and 79.60 ± 0.66 °C. To was associated with hydration and swelling of the amorphous zone inside starch granules (Barichello et al., 1990). In the fermentation process, the degrading of the branched chain of amylopectin resulted in the instability of the amorphous zone (Tian et al., 2024). This may account for the changes of To between fermented and unfermented rice flour. The decrease in To and Tp of the fermented rice flour suggested that the crystal structure of rice flour was disrupted, and crystallinity was reduced after fermentation (Barichello et al., 1990). The ΔH is the energy required from the starch-water system to form a paste (Li et al., 2023) and it indicated the loss of double helix structure during gelatinization (Cooke and Gidley, 1992). The ΔH rose to 9.90 ± 0.24 J/g for the rice flour fermented for 5 days. This implied that more double helix structures were formed in F_5. In rice flour, the protein affected the enthalpy change during starch gelatinization (Park et al., 2020). In the present study, the crude protein content of F_5 was significantly lower ($p < 0.05$) than other samples, and the decreased crude protein content contributed to the increased ΔH of F_5.

3.8. The microstructure of fermented rice flour

The microstructures of fermented rice flour were shown in Fig. 8. The surface of rice flour granules showed a flat and smooth appearance. Interestingly, a certain amount of pores were observed on the surface of the rice flour granules fermented for 2, 3 and 5 days, in which the number of pores showed an increasing trend with the extension of fermentation time, the previous study suggested that the pores were rooted in acid hydrolysis (Govindaraju et al., 2021). In the present study, these pores may be ascribed to the behaviors of organic acids generated by *Lactobacillus plantarum*. Importantly, these pores provided a channel for enzymes to enter the interior of rice flour granules (Govindaraju et al., 2021), which was conducive to degrading the constituents.

4. Conclusions

This study indicated that *Lactobacillus plantarum* fermentation for

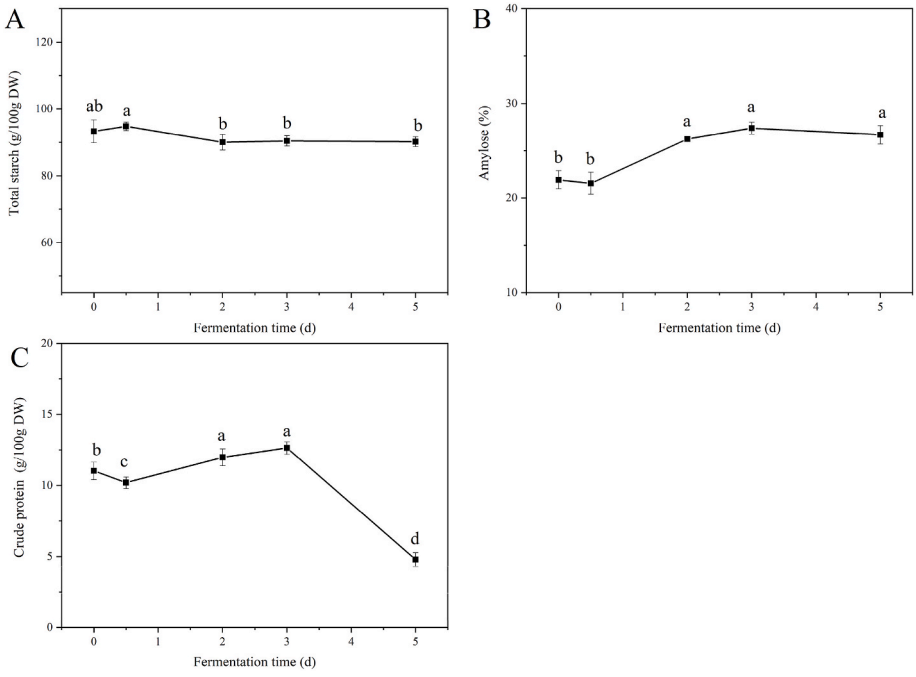

Fig. 6. The evolution of starch and crude protein content of rice flour during fermentation. Values with different lowercase letters indicate significant difference ($p < 0.05$). A indicates starch content. B indicates amylose content. C indicates crude protein content.

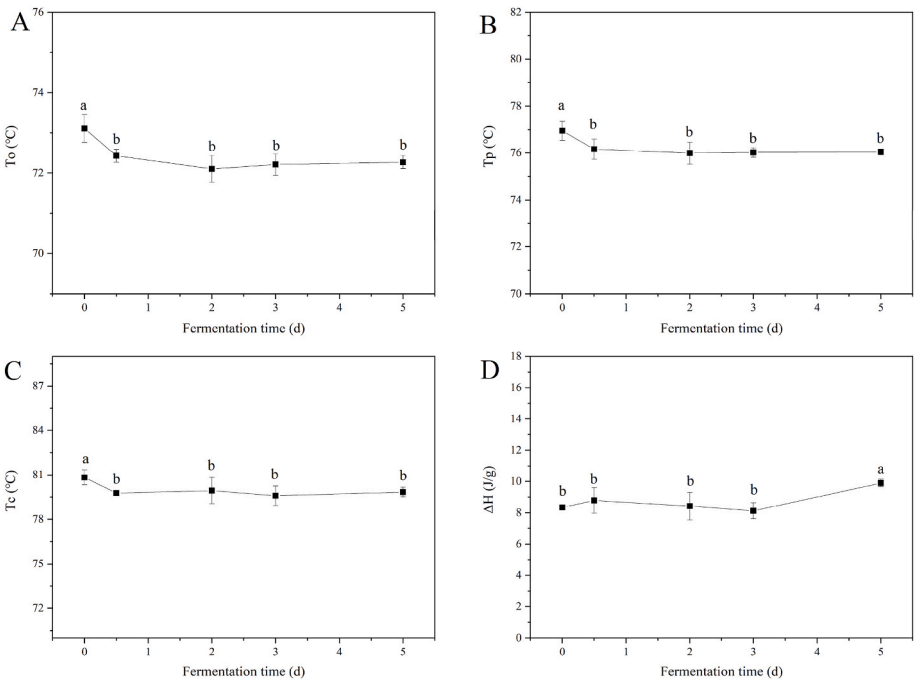

Fig. 7. The evolution of thermal properties of rice flour with the forwarding of fermentation. Values with different lowercase letters indicate significant difference ($p < 0.05$). A indicates the onset temperature (To). B indicates peak temperature (Tp). C indicates conclusion temperature (Tc). D indicates enthalpy change (ΔH).

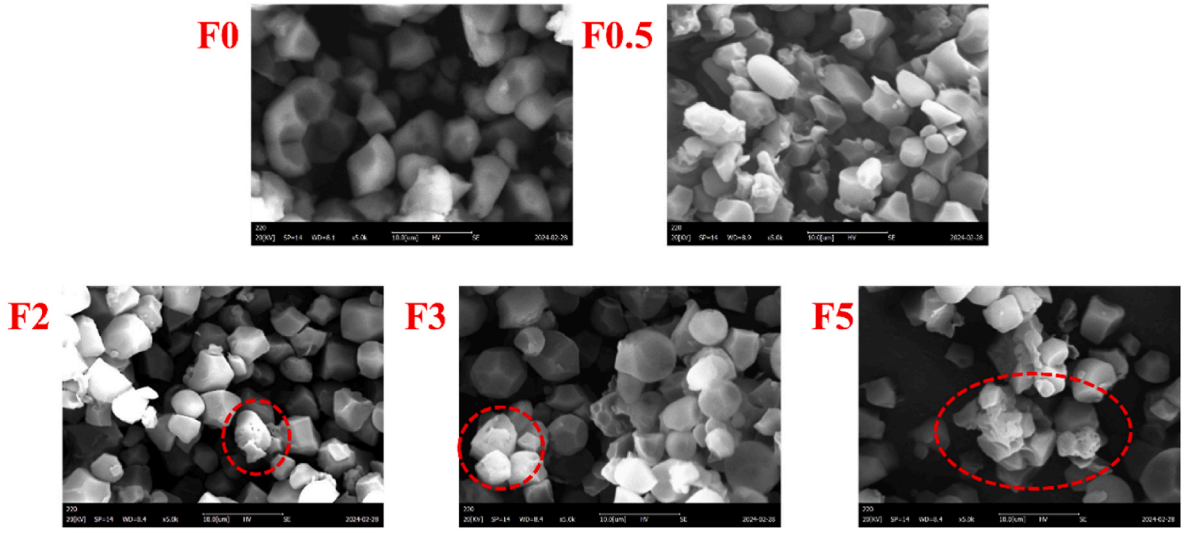

Fig. 8. The microstructure of rice flour granules observed by using scanning electron microscopy.

rice flour intensified the structure of the corresponding rice flour gel by changing the chemical constituents of rice flour and generating organic acids in the fermentation broth. The fermentation process increased the amylose content and decreased crude protein content, both of which were prone to the formation of gel network structure. Moreover, the organic acids generated from *Lactobacillus plantarum* metabolism may contribute to the reinforcing of gel structure by means of hydrolyzing the components on the surface of the rice flour granules, which provides a channel for enzymes to enter the interior of granules.

CRediT authorship contribution statement

Wenmin Ao: Data curation, Formal analysis, Investigation, Methodology, Validation, Visualization, Writing – original draft, Writing – review & editing. **Likang Qin:** Funding acquisition, Resources, Supervision. **Ning Wu:** Funding acquisition, Investigation. **Pingzhen Ge:** Resources, Funding acquisition, Investigation. **Chengmei Hu:** Methodology, Data curation. **Jinlan Hu:** Data curation. **Yujie Peng:** Data curation. **Yong Zhu:** Conceptualization, Funding acquisition, Investigation, Methodology, Project administration, Resources, Supervision, Validation, Visualization, Writing – original draft, Writing – review & editing.

Declaration of competing interest

The authors declare that they have no known competing financial interests or personal relationships that could have appeared to influence the work reported in this paper.

Data availability

Data will be made available on request.

Acknowledgment

This research was financially supported by Guizhou Science and Technology Program, China [Qian Ke He Zhi Cheng (2022) zhongdian 007, Qian Ke He Zhi Cheng (2021) yiban 175]. All authors are grateful to Guizhou Key Laboratory of Agricultural Biotechnology for assisting in rheometer analysis.

References

Ahuja, A., Lee, R., Latshaw, A., Foster, P., 2020. Rheology of starch dispersions at high temperatures. J. Texture Stud. 51 (4), 575–584.
Amagliani, L., O Regan, J., Kelly, A.L., O Mahony, J.A., 2016. Chemistry, structure, functionality and applications of rice starch. J. Cereal. Sci. 70, 291–300.
Barichello, V., Yada, R.Y., Coffin, R.H., Stanley, D.W., 1990. Low temperature sweetening in susceptible and resistant potatoes: starch structure and composition. J. Food Sci. 55 (4), 1054–1059.
Chen, J., Cui, Y., Shi, W., Ma, Y., Zhang, S., 2023. The interaction between wheat starch and pectin with different esterification degree and its influence on the properties of wheat starch-pectin gel. Food Hydrocolloids 145, 109062.
Chen, P., Xie, F., Zhao, L., Qiao, Q., Liu, X., 2017. Effect of acid hydrolysis on the multi-scale structure change of starch with different amylose content. Food Hydrocolloids 69, 359–368.
China, N.H.A.F., Administration, S.F.A.D., 2016a. National Standards of the People's republic of china Method for the Determination of Starch in Food in: GB/5009, pp. 9–2016.
China, N.H.A.F., Administration, S.F.A.D., 2016b. National Standards of the People's republic of china Method for the Determination of Protein in Food in: GB/5009, pp. 5–2016.
Cooke, D., Gidley, M.J., 1992. Loss of crystalline and molecular order during starch gelatinisation: origin of the enthalpic transition. Carbohydr. Res. 227, 103–112.
Dan, H., Gu, Z., Li, C., Fang, Z., Hu, B., Wang, C., Chen, S., Tang, X., Ren, Y., Wu, W., Zeng, Z., Liu, Y., 2022. Effect of fermentation time and addition amount of rice sourdoughs with different microbial compositions on the physicochemical properties of three gluten-free rice breads. Food Res. Int. 161, 111889.
Dang, Y., Imaizumi, T., Nishizu, T., Anandalakshmi, R., Katsuno, N., 2023. Effect of the addition of pregelatinized rice starch paste on the retrogradation of rice starch gel. Food Hydrocolloids 145, 109159.
Dou, X., Ren, X., Zheng, Q., He, Y., Lv, M., Liu, L., Yang, P., Hao, Y., Chen, F., Tang, X., 2023. Effects of lactic acid bacteria fermentation on the physicochemical properties of rice flour and rice starch and on the anti-staling of rice bread. Foods 12 (20), 3818.
Fazeli, Burestan N., Afkari Sayyah, A.H., Safi, M., 2021. Prediction of amylose content, protein content, breakdown, and setback viscosity ofkadus rice and its flour by near-infrared spectroscopy (nirs) analysis. J. Food Process. Preserv. 45 (1).
Freire, A.L., Ramos, C.L., Schwan, R.F., 2017. Effect of symbiotic interaction between a fructooligosaccharide and probiotic on the kinetic fermentation and chemical profile of maize blended rice beverages. Food Res. Int. 100, 698–707.
Geng, D., Liang, T., Yang, M., Wang, L., Zhou, X., Sun, X., Liu, L., Zhou, S., Tong, L., 2019. Effects of lactobacillus combined with semidry flour milling on the quality and flavor of fermented rice noodles. Food Res. Int. 126, 108612.
Govindaraju, I., Chakraborty, I., Baruah, V.J., Sarmah, B., Mahato, K.K., Mazumder, N., 2021. Structure and morphological properties of starch macromolecule using biophysical techniques. Starch Stärke 73 (1–2), 2000030.
Han, W., Zhao, T., Wang, X., 2016. Steady shear viscosity and oscillatory complex viscosity of poly(p-phenylene terephthalamide) solutions in sulfuric acid. Rheol. Acta 55 (3), 257–266.
Holdsworth, S.D., 1971. Applicability of rheological models to the interpretation of flow and processing behaviour of fluid food products. J. Texture Stud. 2, 393–418.
Hung, P.V., Vien, N.L., Lan, Phi N.T., 2016. Resistant starch improvement of rice starches under a combination of acid and heat-moisture treatments. Food Chem. 191, 67–73.
Irani, M., Razavi, S.M.A., Abdel-Aal, E.M., Hucl, P., Patterson, C.A., 2019. Viscoelastic and textural properties of canary seed starch gels in comparison with wheat starch gel. Int. J. Biol. Macromol. 124, 270–281.
Ji, Z., Yu, L., Liu, H., Bao, X., Wang, Y., Chen, L., 2017. Effect of pressure with shear stress on gelatinization of starches with different amylose/amylopectin ratios. Food Hydrocolloids 72, 331–337.
Jiang, B., Li, W., Hu, X., Shen, J., Qun, W., 2013. Rheology of mung bean starch treated by high hydrostatic pressure. Int. J. Food Prop. 81–92.
Karma, V., Gupta, A.D., Yadav, D.K., Singh, A.A., Verma, M., Singh, H., 2022. Recent developments in starch modification by organic acids: a review. Starch Stärke 74 (9–10), 2200025.
Li, C., Yi, X., Yang, C., Li, E., 2023. Starch fine molecular structures as driving factors for multiphasic starch gelatinization property in rice flour. Cereal Chem. 1–14.
Li, H., Prakash, S., Nicholson, T.M., Fitzgerald, M.A., Gilbert, R.G., 2016. Instrumental measurement of cooked rice texture by dynamic rheological testing and its relation to the fine structure of rice starch. Carbohydr. Polym. 146, 253–263.
Li, Q., Li, C., Li, E., Gilbert, R.G., Xu, B., 2020. A molecular explanation of wheat starch physicochemical properties related to noodle eating quality. Food Hydrocolloids 108, 106035.
Lu, Z.H., Peng, H.H., Cao, W., Tatsumi, E., Li, L.T., 2008a. Isolation, characterization and identification of lactic acid bacteria and yeasts from sour mifen, a traditional fermented rice noodle from China. J. Appl. Microbiol. 105 (3), 893–903.
Lu, Z., Cao, W., Peng, H., Wang, F., Tatsumi, E., Kohyama, K., Li, L., 2008b. Effect of fermentation metabolites on rheological and sensory properties of fermented rice noodles. J. Sci. Food Agric. 88 (12), 2134–2141.
Luo, S., Zhou, B., Cheng, L., Huang, J., Zou, P., Zeng, Y., Huang, S., Chen, T., Liu, C., Wu, J., 2022. Pre-fermentation of rice flour for improving the cooking quality of extruded instant rice. Food Chem. 386, 132757.
Majzoobi, M., Beparva, P., 2014. Effects of acetic acid and lactic acid on physicochemical characteristics of native and cross-linked wheat starches. Food Chem. 147, 312–317.
Miles, M.J., Morris, V.J., Orford, P.D., Ring, S.G., 1985. The roles of amylose and amylopectin in the gelation and retrogradation of starch. Carbohydr. Res. 135, 271–281.
Mohammad Amini, A., Razavi, S.M.A., Mortazavi, S.A., 2015. Morphological, physicochemical, and viscoelastic properties of sonicated corn starch, 122, 282–292.
Nie, H., Li, C., Liu, P., Lei, C., Li, J., 2019. Retrogradation, gel texture properties, intrinsic viscosity and degradation mechanism of potato starch paste under ultrasonic irradiation. Food Hydrocolloids 95, 590–600.
Park, J., Sung, J.M., Choi, Y., Park, J., 2020. Effect of natural fermentation on milled rice grains: physicochemical and functional properties of rice flour. Food Hydrocolloids 108, 106005.
Pinhal, S., Ropers, D., Geiselmann, J., de Jong, H., Metcalf, W.W., 2019. Acetate metabolism and the inhibition of bacterial growth by acetate. J. Bacteriol. 201 (13), 1–166.
Punia, Bangar S., Whiteside, W.S., Singh, A., Özogul, F., Gupta, A., Gahlawat, S.K., 2022. Properties, preparation methods, and application of sour starches in the food. Trends Food Sci. Technol. 121, 44–58.
Putseys, J.A., Gommes, C.J., Van Puyvelde, P., Delcour, J.A., Goderis, B., 2011. In situ saxs under shear unveils the gelation of aqueous starch suspensions and the impact of added amylose–lipid complexes. Carbohydr. Polym. 84 (3), 1141–1150.
Rincón-Londoño, N., Millan-Malo, B., Rodríguez-García, M.E., 2016. Analysis of thermal pasting profile in corn starch rich in amylose and amylopectin: physicochemical transformations, part ii. Int. J. Biol. Macromol. 89, 43–53.
Shi, M., Gao, Q., Liu, Y., 2018. Changes in the structure and digestibility of wrinkled pea starch with malic acid treatment. Polymers 10 (12), 1359.
Sikora, M., Krystyjan, M., Dobosz, A., Tomasik, P., Walkowiak, K., Masewicz, A., Kowalczewski, P.A., Baranowska, H.M., 2019. Molecular analysis of retrogradation of corn starches. Polymers 11 (11), 1764.
Tian, J., Qin, L., Zeng, X., Ge, P., Fan, J., Zhu, Y., 2023. The role of amylose in gel forming of rice flour. Foods 12 (6), 1210.
Tian, Y., Liu, X., Kirkensgaard, J.J.K., Khakimov, B., Enemark-Rasmussen, K., Hebelstrup, K.H., Blennow, A., Zhong, Y., 2024. Characterization of different high amylose starch granules. Part i: multi-scale structures and relationships to thermal properties. Food Hydrocolloids 146, 109286.
Tu, Y., Huang, S., Chi, C., Lu, P., Chen, L., Li, L., Li, X., 2021. Digestibility and structure changes of rice starch following co-fermentation of yeast and lactobacillus strains. Int. J. Biol. Macromol. 184, 530–537.
Varela, M.S., Navarro, A.S., Yamul, D.K., 2016. Effect of hydrocolloids on the properties of wheat/potato starch mixtures. Starch Stärke 68 (7–8), 753–761.
Wang, A., Xiao, T., Xi, H., Qin, W., He, Y., Nie, M., Chen, Z., Wang, L., Liu, L., Wang, F., Tong, L., 2022. Edible qualities, microbial compositions and volatile compounds in fresh fermented rice noodles fermented with different starter cultures. Food Res. Int. 156, 111184.
Wang, D., Fan, H., Wang, B., Liu, L., Shi, Y., Zhang, N., 2023. Effects of lactic acid bacteria fermentation on the physicochemical and structural characteristics of starch in blends of glutinous and japonica rice. J. Food Sci. 88 (4), 1623–1639.
Wang, L., Xu, J., Fan, X., Wang, Q., Wang, P., Zhang, Y., Cui, L., Yuan, J., Yu, Y., 2016. Effect of disaccharides of different composition and linkage on corn and waxy corn starch retrogradation. Food Hydrocolloids 61, 531–536.
Wei, P., Fang, F., Liu, G., Zhang, Y., Wei, L., Zhou, K., You, X., Li, M., Wang, Y., Sun, J., Deng, S., 2022. Effects of composition, thermal, and theological properties of rice raw material on rice noodle quality. Front. Nutr. 9, 1003657.
Wu, C., Gong, X., Zhang, J., Zhang, C., Qian, J., Zhu, W., 2023. Effect of rice protein on the gelatinization and retrogradation properties of rice starch. Int. J. Biol. Macromol. 242, 125061.
Xie, H., Gao, P., Lu, Z., Wang, F., Chai, L., Shi, J., Zhang, H., Geng, Y., Zhang, X., Xu, Z., 2023. Changes in physicochemical characteristics and metabolites in the fermentation of goji juice by lactiplantibacillus plantarum. Food Biosci. 54, 102881.
Ye, F., Xiao, L., Liang, Y.N., Zhou, Y., Zhao, G., 2019. Spontaneous fermentation tunes the physicochemical properties of sweet potato starch by modifying the structure of starch molecules. Carbohydr. Polym. 213, 79–88.
Yi, C., Yang, Y., Zhou, S., He, Y., 2017. Role of lactic acid bacteria in the eating qualities of fermented rice noodles. Cereal Chem. J. 94 (2), 349–356.
Zehra, N., Mohsin Ali, T., Mustafa, G., Hasnain, A., 2022. Characterization of citric acid treated partially cold-water swellable sorghum and corn starch extrudates; A green approach. Starch Stärke 74, 2100291.
Zhang, T., Hong, S., Zhang, J.R., Liu, P.H., Li, S., Wen, Z., Xiao, J., Zhang, G., Habimana, O., Shah, N.P., Sui, Z., Corke, H., 2024. The effect of lactic acid bacteria

fermentation on physicochemical properties of starch from fermented proso millet flour. Food Chem. 437, 137764.
Zhu, F., Liu, P., 2020. Starch gelatinization, retrogradation, and enzyme susceptibility of retrograded starch: effect of amylopectin internal molecular structure. Food Chem. 316, 126036.
Ulbrich, M., Terstegen, T.A., Flöter, E., 2019. Molecular investigation of the gel structure of native starches. Starch Stärke 71, 1800080.